

TECHNICAL MEMORANDUM

X-186

TESTS OF AERODYNAMICALLY HEATED MULTIWEB WING STRUCTURES IN A FREE JET AT MACH NUMBER 2

FIVE ALUMINUM-ALLOY MODELS OF 20-INCH CHORD WAT

0.064-INCH-THICK SKIN, 0.025-INCH-THICK WEB

AND VARIOUS CHORDWISE STIFFENING

AT 20 ANGLE OF ATTACK

By Donald H. Trussell and Robert G. Thom

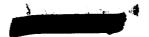
Langley Research Center Langley Field, Va.

CLASSIFIED DOCUMENT - TITLE UNCLASSIFIED

This material contains information affecting the national defense of the United States withing of the espionage laws, Title 18, U.S.C., Secs. 793 and 794, the transmission or revelation manner to an unauthorized person is prohibited by law.

NATIONAL AERONAUTICS AND SPACE ADMINISTRATION January 1960 WASHINGTON

		-



NATIONAL AERONAUTICS AND SPACE ADMINISTRATION

TECHNICAL MEMORANDUM X-186

TESTS OF AERODYNAMICALLY HEATED MULTIWEB WING STRUCTURES

IN A FREE JET AT MACH NUMBER 2

FIVE ALUMINUM-ALLOY MODELS OF 20-INCH CHORD WITH 0.064-INCH-THICK SKIN, 0.025-INCH-THICK WEBS, AND VARIOUS CHORDWISE STIFFENING

AT 20 ANGLE OF ATTACK*

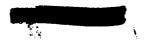
By Donald H. Trussell and Robert G. Thomson

SUMMARY

An experimental study was made on five 2024-T3 aluminum-alloy multiweb wing structures (MW-2-(4), MW-4-(3), MW-16, MW-17, and MW-18), at a Mach number of 2 and an angle of attack of 20, under simulated supersonic flight conditions. These models, of 20-inch chord and semispan and 5-percent-thick circular-arc airfoil section, were identical except for the type and amount of chordwise stiffening. One model with no chordwise ribs between root and tip bulkhead fluttered and failed dynamically partway through its test. Another model with no chordwise ribs (and a thinner tip bulkhead) experienced a static bending type of failure while undergoing flutter. The three remaining models with one, two, or three chordwise ribs survived their tests. The test results indicate that the chordwise shear rigidity imparted to the models by the addition of even one chordwise rib precludes flutter and subsequent failure under the imposed test conditions. This paper presents temperature and strain data obtained from the tests and discusses the behavior of the models.

^{*}Title, Unclassified.





INTRODUCTION

The Langley Structures Research Division has been engaged in an investigation to determine the effects of aerodynamic heating on aircraft structures. As part of this investigation, a series of multiweb wing structures has been tested in a free jet at a Mach number of 2. These multiweb models had 5-percent-thick circular-arc airfoil sections and solid leading and trailing edges.

The first of these models, designated as MW-1, was an aluminum-alloy wing of 40-inch chord and semispan and was instrumented only with thermocouples. The test of this model was conducted to obtain skin and internal temperature variations with time. However, the aerodynamic heating and loading caused the model to flutter and fail near the end of the test. The results of the test of model MW-1 are presented in reference 1.

Subsequent models were similar to model MW-l in design, but had 20-inch chords and semispans with the exception of MW-l-(2), a duplicate of MW-l, which had more thermocouple instrumentation than MW-l and also had some strain-gage and pressure instrumentation. The 20-inch models differed in internal structure, skin thickness, and material. The results reported thus far on tests of these models can be found in references 2 to 8.

This paper presents the results for five models tested at 2° angle of attack and at a Mach number of 2 with sea-level static temperature and pressure. These models, designated as MW-2-(4), MW-4(3), MW-16, MW-17, and MW-18, varied only in the type and amount of chordwise stiffening. Model temperatures and strains were measured and high-speed motion pictures were taken during all tests.

SYMBOLS

а	speed of sound, fps
ı	distance along model chord from leading edge, f
М	Mach number
р	pressure, psia
q	dynamic pressure, $\frac{1}{2}\rho V^2$, psi





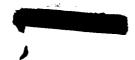
R	Reynolds number per foot, $\frac{\rho V l}{\mu}$
t	time from start of air flow, sec
T	temperature, ^O F
V	velocity of air, fps
α	angle of attack, deg
μ	absolute viscosity of air, slugs/ft-sec
ρ	density of air, slugs/cu ft
Subscript	s:
aw	adiabatic wall
0	initial conditions
t	tunnel stagnation conditions
∞	free-stream conditions

MODELS AND TESTS

Model Construction

All the models in the group reported in this paper were of the same exterior configuration (20-inch chord and semispan and 5-percent-thick symmetrical circular-arc airfoil) and all were fabricated of 2024-T3 aluminum alloy. All models had solid leading and trailing edges and six 0.025-inch-thick formed, spanwise stiffeners and 0.064-inch-thick skins. The models were also identical in the design of the root section, with a solid root bulkhead and doubler plates to strengthen the root connection. Figure 1 shows the construction details of the models. Section AA shows details of the tip bulkheads, and section BB (fig. 1(a)) shows the root construction and attachment to the model mounting support.

The only difference in the design of the models was the type and amount of chordwise stiffening. Model MW-2-(4) had an 0.250-inch-thick solid tip bulkhead, whereas models MW-4-(3), MW-16, MW-17, and MW-18 had 0.025-inch-thick formed tip bulkheads. Also, models MW-2-(4) and MW-4(3) had no internal chordwise ribs whereas models MW-16, MW-17,





and MW-18 had three, two, and one chordwise ribs, respectively. These ribs had the same dimensions as the tip bulkheads of models MW-4-(3), MW-16, MW-17, and MW-18, but were discontinuous at the spar webs. (See fig. 1(c).)

After the models were assembled, they were painted with a thin coating of zinc chromate primer and striped with black lacquer to form a grid pattern which aided in studying the model behavior recorded by the motion-picture films.

Model Instrumentation

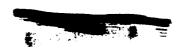
Instrumentation consisted of thermocouples and wire strain gages installed at the locations noted in figure 2. Figure 3 shows the straingage and thermocouple instrumentation and the internal structure of model MW-16 prior to final assembly. Much of the instrumentation for models MW-16, MW-17, and MW-18 (fig. 2) was inoperative for the tests reported herein because of damage incurred in previous tests.

Iron-constantan thermocouples were installed in the skins and stiffeners by forming a common bead on one end of the thermocouple lead wires and peening the bead into a hole drilled to the midplane of the material at the desired location. Thermocouples located in the interior of the solid leading- and trailing-edge sections (MW-16) were installed by coating the hot-junction beads with cement and inserting the beads into small holes drilled into those sections.

The model strain gages were SR-4 type EBDF-7D temperature-compensated wire strain gages and were attached to the models with thermosetting cement. These gages are temperature-compensated to read approximately zero strain on unstressed 2024-T3 aluminum alloy at temperatures between 50° F and 250° F. A detailed explanation of the strain-gage installation technique and temperature compensation is discussed in reference 7.

Accuracy of Data

The estimated probable errors in individual measurements of the model and tunnel instrumentation, and the corresponding time constants are presented in the following table:





Item	Probable error	Time constant, a sec
Tunnel stagnation pressure Tunnel stagnation temperature	±30 F	0.03 0.12 0.03 0.02

^aThe time constant is defined to be the time required for a recorded value to reach 63 percent of a step-function input value. The determination of the time constant is independent of the probable error.

Errors that result from the hot-junction thermocouple installation have not been evaluated and are not included in the probable error, but these errors are believed to be small. These hot-junction errors can result from variations in the contact pressure between the thermocouple bead and the model skin when the model skin is vibrating, or in the case of the thermocouples in the leading and trailing edges of model MW-lo, the errors can result from the insulating effect of the cement used in the installation.

Vibration Nodal Patterns and Frequencies

Prior to the aerodynamic tests, the models were subjected to vibration surveys to determine their natural nodal patterns and corresponding frequencies at room temperature. (Models MW-16, MW-17, and MW-18 were previously surveyed. See ref. 7.) An air-jet shaker was used to excite the models and the vibrations were received by a velocity pickup and circuited to a cathode-ray oscilloscope. The velocity pickup was moved over the surface of a model to determine the node lines; frequencies were measured by a Stroboconn frequency meter. Figure 4 shows the results of these surveys. The nodal patterns (fig. 4) are composites for all models; individual model node lines varied slightly.

Although the five models were outwardly identical, they were different structurally; therefore, their natural modes and frequencies might be expected to be dissimilar. The lightest model, MW-4-(3), which had a light tip bulkhead and no ribs, can be used as a basis of structural comparison since the remaining models varied either by having a heavier tip rib (MW-2-(4)) or by the addition of one, two, or three ribs (MW-18, MW-17, or MW-16). The heavier tip bulkhead of model MW-2-(4) (over that of model MW-4-(3)) resulted in no significant difference in either the nodal patterns or corresponding frequencies (except for pattern K of fig. 4); any additional stiffness near the tip of the wing was apparently offset dynamically by the added mass.



Since the two models without ribs responded similarly over the frequency range covered by this survey, another comparison can be made between the models without ribs and those having ribs. The lowest frequency of the first mode involving primarily chordwise distortion for the rib-stiffened models (nodal pattern I) was 450 cps, whereas, for the models with no ribs, the frequencies were less than 280 cps (nodal pattern C). The addition of ribs to the basic model design (MW-4-(3)) changed nodal pattern C from a mode involving primarily chordwise distortion to nodal pattern D, a mode involving primarily bending distortions. Also, over the frequency range of this survey, the models without ribs experienced more chordwise distortion modes than were experienced by the rib-stiffened models. Therefore, as expected, the models without chordwise ribs were considerably less resistant to chordwise distortions than were the rib-stiffened models. Moreover, the addition of one rib to the basic model design is sufficient to preclude natural modes involving primarily chordwise distortion in the frequency range below 450 cps.

The results shown for models MW-16, MW-17, and MW-18 differ only slightly from previous results for these models reported in reference 7. In general, the modal frequencies reported herein are lower than those reported in reference 7. These lower frequencies probably indicate a reduction in stiffness resulting from repeated testing of these models.

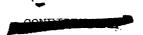
Test Facility

The facility used for the aerodynamic tests of the multiweb wing models was the preflight jet of the NASA Wallops Station. This facility is a supersonic, blowdown jet which utilizes a heat accumulator for stagnation-temperature control. Models were tested in a free jet at a Mach number of 2 downstream of the exit of the 27- by 27-inch nozzle. This facility and its operation are discussed in the appendix of reference 2.

Test Procedure

Model mounting. The models were mounted root downward at an angle of attack of 2^{O} with the leading edge approximately 2 inches downstream of the nozzle exit plane. Figure 5 shows a typical model in test position at the exit of the 27- by 27-inch jet. (The two stagnation-temperature probes located to the rear of the model were not used for the tests discussed in this paper.) The angle of attack is noted as positive for clockwise rotation looking down on the tip of the model. The models were pivoted about a point $2l\frac{1}{2}$ inches downstream of the





leading edge. The angle of attack was measured between the exit plane of the jet and the tip chord line of the model.

An aerodynamic fence surrounded the models near the root so that only $19\frac{7}{8}$ inches of the total semispan of $24\frac{1}{8}$ inches were exposed to the supersonic airstream. The sharp leading edge of the aerodynamic fence was positioned 1/8 of an inch above the lower jet boundary to remove some of the cold boundary layer. (See fig. 2.)

Supporting equipment.— The sequencing of the supporting equipment required for any test was accomplished with a programing device. The photographic lighting, time-correlating device, cameras, data recorders, and also the opening of the pressure control valve were individually energized on signal from the programer. The temperature, pressure, and strain data were recorded on three 18-channel recording oscillographs.

In the tests, five motion-picture cameras were focused on the models from various positions to record the model behavior. Two of these cameras were run at a film speed of 110 frames per second throughout the test, a third was run at a film speed of 1,000 frames per second throughout the test, and each of the remaining two cameras was sequenced to record approximately half a test at 1,600 frames per second.

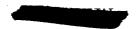
Test Conditions

Test conditions were considered to exist when the tunnel stagnation pressure exceeded 100 psia - the pressure required to establish supersonic flow over the entire model. For the tests on each of the five models, the tunnel stagnation pressures are plotted in figure 6(a) and the stagnation temperatures in figure 6(b). The average test stagnation pressures and temperatures presented in table 1 were obtained by integration of the area under the stagnation pressure and temperature curves shown in figure 6 for the interval when the stagnation pressure exceeded 100 psia. The dashed lines shown on the curves represent the average values thus obtained for the time interval in which test conditions were considered to exist. Zero time in all tests was referenced on all data records to the initial disturbance of a static-pressure pickup located slightly upstream from the nozzle exit plane.

The time of initial failure for models MW-2-(4) and MW-4-(3) is shown in figure 6 by the intersection of the vertical line and the pressure or temperature curve.

Table 1 presents the average aerodynamic test conditions determined from the Mach number, the average stagnation temperature, and the average stagnation pressure for the five tests discussed herein. The values





for stagnation pressure and temperature shown in parentheses in table 1 for models MW-2-(4) and MW-4-(3) are the values that prevailed at the time of initial failure of these models.

RESULTS AND DISCUSSION

Model Temperatures

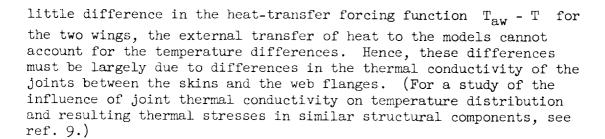
Temperature data. The temperature data at 1-second intervals for the five model tests discussed in this paper are presented in table 2. The data indicate that all tests were of a transient nature and hence insufficient in length for the models to reach steady-state temperatures. The data also show the characteristic temperature variations exhibited in previous multiweb wing tests in this jet facility. These variations indicate that a spanwise temperature gradient in the jet results in higher temperatures near the tip and midspan than near the root. The data also show a characteristic chordwise decrease in skin temperature from leading to trailing edge at any given time, due to a decrease in aerodynamic heat transfer with chord length. The amount of temperature data obtained was limited because of the larger thermocouple fatality.

Skin-web temperature differences. The skin and web temperatures for models MW-2-(4) and MW-4-(3) at 2 seconds of test time have been plotted in figure 7. The temperature data for models MW-16, MW-17, and MW-18 were not plotted because the models did not fail and, unlike models MW-2-(4) and MW-4-(3), the data were obtained from very dissimilar locations and after repeated previous tests.

Figure 7 shows the temperatures, expressed nondimensionally to allow direct comparison, at corresponding skin and web center-line locations for models MW-2-(4) and MW-4-(3). Although there is considerable scatter in the data, the differences between the temperatures at the web center lines and the model skin temperatures (at locations where there was essentially no conduction to the stiffeners) can be seen, in general, to be appreciably greater for model MW-4-(3) than for model MW-2-(4); thus, it is reasonable to expect that the thermal stresses were also greater. (The actual thermal stress at a point is a function of the temperature difference between the weighted average temperature and the temperature of the point.)

The larger temperature differences for model MW-4-(3) might be attributed either to differences in the imposed test heating conditions or to normal fabrication differences in the models, such as differences in the joints. However, since the aerodynamic heat-transfer coefficients should have been almost identical, and since there was also very





Model Strains

The model strain data at 1-second intervals are shown in table 3 exactly as they were reduced from the oscillograph records, i.e., without any temperature corrections. Where data are not given in this table, either the strain gage was inoperative or large oscillations in the oscillograph record prevented reading the data.

All the strain gages installed in models MW-2-(4) and MW-4-(3) except gages 8 and 9 were intended to be used to record the frequency of vibrations and allow phasing of any chordwise distortions; gages 8 and 9 were intended to yield strain histories in bending about the root. The results shown in table 3 for these two models serve only to show the relative magnitude of the recorded strains in the area of the gages. Although the gages experienced high-amplitude vibrations at frequencies above the flat frequencies of the galvanometers, the phasing analysis is believed to be reliable because the vibrations were nearly equal in frequency and the attenuation in the signals from the gages should have been approximately the same.

The strain gages installed in models MW-16, MW-17, and MW-18 were also intended primarily to record frequency histories; in addition, a few gages were mounted in pairs at right angles to one another to yield biaxial strains so that the local stresses could be approximated at these locations. Also, some single gages were installed on the skin opposite the right-angled pairs and alined with one of the gages to indicate the corresponding strains in the opposite skin. Although 12 pairs of gages were installed in models MW-16, MW-17, and MW-18 to record biaxial strains, only four pairs were operative in these tests (one pair in MW-16, one pair in MW-17, and two pairs in MW-18). The strain gages in models MW-16, MW-17, and MW-18 experienced low-frequency, low-amplitude vibrations; thus, the recorded strains should have been influenced only to a minor degree by such factors as attenuation. However, determination from the strain-gage histories of the true strains experienced by the models is subject to several sources of error, such as temperature compensation for zero drift of the gages. Because of this and other sources of error and because only four pairs of





perpendicular gages were operative, no experimental stress data are presented. Similarly, no calculated stress data are included. Stresses derived from the limited biaxial strain data were generally in fair agreement with stresses calculated by using approximate methods for determining thermal stresses and stresses due to loads.

Model Behavior

All five models were tested under fairly similar conditions, as can be seen from table 1. However, as might be expected from the known physical differences in the models (fig. 1), the wings behaved somewhat differently. Models MW-2-(4) and MW-4-(3), without any internal chordwise stiffening, failed, whereas the three models with internal chordwise ribs did not. A brief summary of the significant events which occurred during the tests is given in table 4, and these events are discussed in the following sections. One occurrence, common to all these tests, was that exhibited during the starting phase of the jet wherein the models were subjected to random pressure distributions and reacted by undergoing large bending deflections coupled with some smaller torsional deflections. Because of these disturbances and similar disturbances which occur during shutdown, repeated testing (as, for example, the previous tests of models MW-16, MW-17, and MW-18) could result in damage to the models and to instrumentation; however, although much of the original instrumentation in these models was inoperative, no damage to the model structure was evident prior to the tests. The behavior of all models and the times of the various events were obtained by correlating the strain-gage data with the high-speed motion pictures.

A motion-picture film supplement has been prepared of the tests on models MW-2-(4) and MW-4-(3) and is available on loan. A request card form and a description of the film will be found at the back of this paper, on the page immediately preceding the abstract and index pages.

Model MW-2-(4).- As indicated in table 4, model MW-2-(4) began to flutter at 1.77 seconds, just after the desired test conditions had been established. The flutter occurred at a frequency of 480 to 500 cps, was of small amplitude with five spanwise node lines across the chord, and included only slight distortion of the tip bulkhead. This initial flutter mode of $2\frac{1}{2}$ waves was different from the $1\frac{1}{2}$ -wave flutter mode observed before failure on similar models in this test series tested at 0° angle of attack (ref. 5). Tests of model MW-2-(2) at angles of attack of -2° and 2° (runs 4 and 6 of ref. 4) revealed a low-amplitude flutter at 360 to 400 cps. Although an accurate description of the flutter mode cannot be determined for model MW-2-(2) from the highspeed motion pictures because of the small amplitude of vibrations and





lack of clarity of the films, the flutter mode appears to be similar to the initial flutter mode described herein for model MW-2-(4).

As in similar tests where failure due to flutter had occurred, the amplitudes increased appreciably before failure, especially near the trailing edge. At 5.01 seconds, failure occurred when the rivets connecting the fifth web (from the leading edge) and the skin failed. Shortly thereafter the mode changed to the more usual $1\frac{1}{2}$ waves across the chord, the amplitudes increased considerably, and the frequency dropped to about 200 cps. At 5.79 seconds, the wing tore away completely from its root attachment.

Model MW-4-(3).- The behavior of model MW-4-(3) was quite similar to that of model MW-2-(4) until failure occurred, except that flutter began slightly sooner, at 1.50 seconds (table 4). However, this wing experienced a static bending type of failure at 2.56 seconds by collapse at the root while undergoing flutter at approximately 480 cps.

Models MW-16, MW-17, and MW-18. Models MW-16, MW-17, and MW-18 behaved similarly during their tests in that the models experienced very low-amplitude vibrations with frequencies of from 45 to 70 cps during the period of test conditions. All three models survived the tests with no apparent physical damage. Thus, since essentially the same aero-dynamic loading and heating were imposed on all five models, the additional chordwise stiffness obtained by adding one, two, or three internal chordwise ribs apparently sufficed to prevent flutter and subsequent failure.

Failures of models MW-2-(4) and MW-4-(3).- One apparent structural difference between models MW-2-(4) and MW-4-(3) was in the tip bulkheads; model MW-2-(4) had a solid 1/4-inch-thick tip bulkhead, whereas model MW-4-(3) had a light, formed bulkhead 0.025 inch thick. The effect of this difference in chordwise bending stiffness at the tip may have resulted in the slightly earlier flutter of model MW-4-(3). A second difference was in the amount of built-in twist (less than 0.5° for either model) which raised the aerodynamic pressure loading on model MW-2-(4) very slightly over that on model MW-4-(3). A third difference was in the thermal conductivity of the joints of the two models; as seen from figure 7, this resulted in larger skin-web temperature differences for model MW-4-(3), and consequently in larger thermal stresses.

Both models began to flutter after test conditions had been established (i.e., after the stagnation pressure exceeded 100 psia) and their flutter behavior was very similar. However, the onset of flutter occurred slightly earlier for MW-4-(3) than for MW-2-(4), and the time and manner of failure of these models were different. These differences in the failures probably were a result of thermal stresses induced by





aerodynamic heating. Because of the lower joint conductivity of model MW-4-(3), the increase of thermal stress with time was more rapid for this model than for model MW-2-(4). A state of critical stress was apparently reached in model MW-4-(3) at 2.56 seconds, at which time the combined stresses due to aerodynamic loading and aerodynamic heating caused skin buckling and collapse. However, for model MW-2-(4), the increase in thermal stress was considerably more gradual and the effect was less severe.

SUMMARY OF RESULTS

Aerodynamic tests were performed on five multiweb wing models at 20 angle of attack in a Mach number 2 free jet under simulated supersonic flight conditions at sea-level static temperature and pressure. Model temperatures and strains were measured and high-speed motion-picture cameras were used to photograph the model behavior. Because of uncertainties in converting the strain data to stresses, the straingage histories were used only to aid in reconstructing the behavior of the models.

The model temperature data revealed that all tests were of a transient nature. The amount of temperature data obtained was limited because of the large thermocouple fatality.

Model MW-2-(4) fluttered and failed partway through its test. Model MW-4-(3) experienced a static bending type of failure at the root while undergoing flutter.

The flutter mode of $2\frac{1}{2}$ waves exhibited by models MW-2-(4) and MW-4-(3) in these tests (at 2° angle of attack) was different from the $1\frac{1}{2}$ -wave flutter mode exhibited by similar models in this test series at 0° angle of attack. However, previous tests of model MW-2-(2) made at an angle of attack of -2° and 2° (NACA RM L57H19) revealed a low-amplitude flutter mode which appears to be similar to the $2\frac{1}{2}$ -wave flutter mode discussed herein for models MW-2-(4) and MW-4-(3).

Models MW-16, MW-17, and MW-18, which had internal chordwise ribs between the root and tip bulkhead, survived the tests without apparent structural damage.

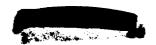
The tests of the five models indicate that small differences in model construction appreciably affect the model behavior and that the addition of one or more chordwise ribs apparently stiffens the design

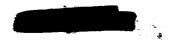




sufficiently to prevent chordwise distortions, flutter, and subsequent failures similar to those experienced by models MW-2-(4) and MW-4-(3) under these test conditions.

Langley Research Center,
National Aeronautics and Space Administration,
Langley Field, Va., August 26, 1959.





REFERENCES

- 1. Heldenfels, Richard R., Rosecrans, Richard, and Griffith, George E.:
 Test of an Aerodynamically Heated Multiweb Wing Structure (MW-1)
 in a Free Jet at Mach Number 2. NACA RM L53E27, 1953.
- 2. Griffith, George E., Miltonberger, Georgene H., and Rosecrans, Richard: Tests of Aerodynamically Heated Multiweb Wing Structures in a Free Jet at Mach Number 2 Two Aluminum-Alloy Models of 20-Inch Chord With 0.064- and 0.081-Inch-Thick Skin. NACA RM L55F13, 1955.
- 3. Rosecrans, Richard, Vosteen, Louis F., and Batdorf, William J., Jr.: Tests of Aerodynamically Heated Multiweb Wing Structures in a Free Jet at Mach Number 2 - Three Aluminum-Alloy Models and One Steel Model of 20-Inch Chord and Span With Various Internal Structures and Skin Thicknesses. NACA RM L57HO1, 1957.
- 4. Miltonberger, Georgene H., Griffith, George E., and Davidson, John R.:
 Tests of Aerodynamically Heated Multiweb Wing Structures in a Free
 Jet at Mach Number 2 Two Aluminum-Alloy Models of 20-Inch Chord
 With 0.064-Inch-Thick Skin at Angles of Attack of 0° and ±2°.
 NACA RM L57H19, 1957.
- 5. Heldenfels, Richard R., and Rosecrans, Richard: Preliminary Results of Supersonic-Jet Tests of Simplified Wing Structures. NACA RM L53E26a, 1953.
- 6. Griffith, George E., and Miltonberger, Georgene H.: Tests of Aero-dynamically Heated Multiweb Wing Structures in a Free Jet at Mach Number 2 An Aluminum-Alloy Model of 40-Inch Chord With 0.125-Inch-Thick Skin. NACA RM L58C24, 1958.
- 7. Davidson, John R., Rosecrans, Richard, and Vosteen, Louis F.: Tests of Aerodynamically Heated Multiweb Wing Structures in a Free Jet at Mach Number 2 Four Aluminum-Alloy Models of 20-Inch Chord and Span With 0.064-Inch-Thick Skin, 0.025-Inch-Thick Ribs and Webs, and Zero, One, Two, or Three Chordwise Ribs. NACA RM L57L13, 1958.
- 8. Davidson, John R., and Rosecrans, Richard: Tests of Aerodynamically Heated Multiweb Wing Structures in a Free Jet at Mach Number 2 Three Models of 20-Inch Chord and Span Constructed From Magnesium, Titanium, and Aluminum Alloys, Respectively. NASA MEMO 10-12-58L, 1958.
- 9. Griffith, George E., and Miltonberger, Georgene H.: Some Effects of Joint Conductivity on the Temperatures and Thermal Stresses in Aero-dynamically Heated Skin-Stiffener Combinations. NACA TN 3699, 1956.



TABLE 1

AERODYNAMIC TEST CONDITIONS

$$\left[\alpha = 2^{\circ}; M = 1.99\right]$$

Feynolds number	per foot,	12.87 × 10 ⁶	13.30	12.39	12.95	13.04
Speed of sound,	a, fps	1,163	1,150	1,177	1,158	1,148
Free-stream Free-stream Speed of velocity, density, sound,	$ ho_{\infty}$, slugs/cu ft	2.22 × 10-3 1,163	2.28	2.15	2.23	2.23
Free-stream	V_{∞} , fps	5,514	2,288	2,342	2,304	2,285
Free-stream Free-stream static dynamic temperature,	다 80 전	104	91	117	98	68
Free-stream dynamic	gω, gω, psi	ተተ. ፲4	41.58	16.04	41.03	24.04
Free-stream static	Po, psia (a)	14.95	15.00	14.76	14.80	14.60
Stagnation temperature,	$^{\mathrm{T}_{t}},$ $^{\mathrm{O}_{\!F}}$	(551)	(531)			
Sta		558	535	574	540	524
tagnation pressure,	Pt, psia (a)	(114.3)	(116.8)			
Stagnation pressure,	Pt ps: (a)	117.8	117.2	113.7	114.0	112.5
	Run	н	-	9	K	3 1
F©st	Model	MM-2-(4) 1 117.8 (114.5) 558 (551)	MW-4-(3) 1 117.2 (116.	MW-16	MW-17	MW-18



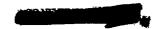


TABLE ?

MODEL TEMPERATURES

Time,													ı illiğə i	gvat.u.	rr, '	°F a	t the	rmo	гочр	le ^a .	-											
sec	1	2	3	4	5	ь	7	8	9	10	11	12	13	1.4	15	16	17	18	19	20	21	22	23	24	25	26	27	28	29	33	34	3 5
	т—					,	, -	,		r				Мос	iel i	W-2	-(4)	,	,				·	r	,		,		,	,	r	
0 1 2 3 4 5	72 89 145	73 121 213	71 76	72 113 172 205 244 293	74 121 198	71 75 125	73 104 139 169 209 253	74 117	72 107 178	71 95 141 206 250	71 73 114	γ2 115	75 112 160 294 294 294	71 73 113	74 114	70 75 111 168 229 221	74 114 200	74 112	71 76 171	72 112	71 85											
	,			,.		·				, .	•			Мос	iel i	W-4.	-(3)	<u> </u>														
0 1 2	52 67 113		50 58 74		州 101 171	54 57 79	54 92 164		50 88 144	94 78 126	53 56 73	5 3 98 170	57 97 160	51 55 73	54 95 168	51 57 76	53 92 166	57 94 166	100 56 100	52 9 3 165	51 62 101											
	T	T	T		1	,	T					,		Мо	odel	MW-	16						,	·				-				
0 1 2 3 4 5 6 7 8 9 10 11 12 13 14 15	249 310 356 383 414 436 451 469 475 475	190 248 299 340 375 403 424 441 453 464		219 301 356 394 423 442	216 257 287 309 324 339 348 356 363										179 235 277 311 339 362 396 417 424 431 418	324 334 342 349 354 354 352	152 199 232 259 279 296 309 319 327 333 336 326	227 249 267 283 296 308 318 325	381 400 416 428 437 442 445 445	146 178 209 238 265 289 310 329 344 360 373	179 211 240 268 293 315 334 350					336 354 369 386 395	239 266 290 313 332 349 365 380 397 403	202 236 265 290 313 332 349 364 378 408	144 267 302 357 357 358 399 406 412 417 422 390			
														Mo	odel	MW-	17															
5 4 5 6 7 8 9	389 405 433 445 461 463 465	319 321 331 338 343 346	255 254 272 288 301 309 318 326		263 284 300 313 323 330 335 338 338 332	87 115 150 181 205 230 250 268 283 294 303	153 198 231 260 277 294 307 317 325 331 535 335 329			64 67 83 114 155 196 235 272 303 331 355 374 389 401 412 414		75 74 85 104 131 157 183 206 225 243 259 273 284 291 295 302	285 320 350 374 408 421 437 443 433			267 304 330 355 375 392 405 417 429 429	158 215 259 293 322 348 367 385 400	240 288 323 353 377 396 413 425 444 444 444	345 370 390 406 420 431 439 442 444			144 184 215 239 256 273 285 295 304 311 318 316	301 308 309 295 294			126 151 175 198 217 234 249 261 272 280 284	73 100 142 181 211 234 253 269 283 293 301 307 314 314 313			214 229 241 310 332 353 370 385 406 418	288 310 329 347 360 372 385 399 384	70 96 139 175 202 221 255 267 278 286 298 298 298 298 296 293
			· · · ·								·			Мо	del	MW - 1	L8															
0 1 2 5 6 7 8 9 10 11 12 13 14 15		67 95 136 176 204 226 254 263 277 283 278 278 276 276	The second secon						317 347 371 391 407 418 427 433 438	64 99 156 208 252 285 311 332 349 362 372 385 386 387 385	215 242 262 277 289 300 306 312 315 308	168 217 258 293 323 347 368 382 393 403	120 145 171 198 226 251 275 296 314 336	167 201 235 269 296 321 341 358 377		78	224 268 307 336 359 378 393 404 414 422 428 419				65 103 168 229 277 314 345 368 387 405 445 445 445 445 445 445 445 445 445		260 297 326 349 369 384 394 402 415 415	68 97 147 193 234 266 291 313 355 363 363 373 372 373	203 229 248 263 276 286 294 300 303 299 301	187 211 230 246 257 268 277 280 272 266 270	103 124 145 170 195 219 243 262 281 306 339	178 150 170 188 205 221 234 245 253 260			65, 96 161 200, 254 264 289, 3513 351, 3548 362, 374 590, 386 385, 385	211 227 241 254 263 272 279 282 278 279

Where data for a particular thermocouple are not given, thermocouple was not in proper working condition at time of cest, where data are listed for only part of test, values beyond those given were considered surveilable.



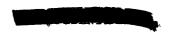


TABLE 5

MODEL STRAIN HISTORIES

Time,							Sta	win,	μ in./	(in., :	ul styni	n property	-					
sec	1	2	3	4	5	6	7	8	9	10	11	12	13	14	16	17	20	21
					•				Model Mw	1-2-(4))	1	·	1				
0 1 2 3 4 5	3 967 409	116 116	-2 476 558 594 626 5 3 6	-9 52 59 182 196 140	7 22 225 618 789 813	-10 -67 -62	0 -29 -555 931 880 540	5 -661 -952 -726 -290	0 8/7 1,703 1,686 1,703	5 -96 -84 884	.8 -102	2 -169 -555	-2 -191 801	4 -154 198				
	,		,					M	lodel Mw	1-4-(3)		•						
0 1 2	-7 707 714	-15 67 5 3	0 529 636	-4 81 171	-3 78 31 5	-53 -53 -53	-41 -57 -623	0 -634 309	17 894 1,995	-14 -75 -113	-7 -72 234	-2 -122 275	2 -166 266	-7 -93 123				
									Model M	W-16	•				•			
0 1 2 5 4 5 6 7 8 9 10 11 12 13 14 15				-2 199 759 758 660 616 537 482 436 399 431 359 253 121 -31		15 235 430 590 602 500 368 225 -38 -184 -225 -288 -355 -418 -466			9 228 1,469 1,488 1,313 1,211 1,103 1,395 1,242 1,089 916 696 587						9 65 104 1154 160 140 115 78 39 -20 -99 -89 -114 -45 -97			
									Model M	W-17								
0 1 2 5 4 5 6 7 8 9 10 11 12 15 14 15	-5 561 501 530 519 517 521 516 569 579 580 526 495 608 352 335		-22 81 106 141 183 277 179 107 79 70 48 19	19 194 457 603 641 611 562 507 453 400 345 293 225 113 47 21		-27 189 21 21 31 26 -5 -23 -15 -18 5 65 26 -65 40 -3		14 -38 -45 -104 -139 -138 -145 -86 -25 -21 -21 -21 -25 -289 186 152	2 -24 323 251 282 252 252 345 381 400 414 394 -18 118	-9 -113 -376 -480 -570 -646 -692 -727 -732 -774 -776 -811 -776 -767 -615 -603	12 118 1,267 1,288 1,278 1,271 1,262 1,265 1,290 1,251 1,191 1,018 805 497 -54 -133	27 -36 -1,044 -1,102 -1,120 -1,132 -1,136 -1,154 -1,125 -1,088 -941 -751 -381 32				10 -10 153 166 153 151 145 151 164 164 184 201 189 240 270 255		
									Model M	W-18								
0 1 2 3 4 5 6 7 8 9 10 11 12 13 14 15				29 133 419 433 476 498 520 527 541 536 513 430 279 181 10 3		25 (283 (244 685) 732 762 664 664 664 664 293 191 83 -23 -70				-17 -85 -358 -484 -573 -623 -715 -715 -715 -812 -708 -678 -673	10 299 1,045 1,110 1,200 1,191 1,203 1,211 1,227 1,222 1,152 1,011 825 304 221 207	0 -38 -468 -549 -472 -455 -510 -182 -183 -176 -15 357 111					44 -22 -173 -265 -353 -406 -440 -511 -529 -558 -419 -358 -371	16 89 344 326 342 316 323 324 316 248 154 118 -66 -45

Amegative sign indicates compressive strain; when the strain gages recorded oscillating strains, the mean value is presented here; where data are not given, either the strain gage was inoperative or large oscillations in the oscillograph record prevented reading the data.





SUMMARY OF MODEL BEHAVIOR

TABLE 4

Model	Time, sec	Event
MW-2-(4)	0.26 to 0.99 0.99 to 1.72 1.77 1.83 4.98 5.01	Random vibrations due to jet starting Model steady Small-amplitude, five-noded mode flutter at 480 to 500 cps Increase in flutter amplitude Marked increase in flutter amplitude near trailing edge First structural (rivet) failure; mode changed to 1½ chordwise waves and fre-
	5.79	quency to 400 cps, then gradual decrease in frequency to 200 cps Wing tore away completely at root
MW-4-(3)	0.26 to 0.99 0.99 to 1.50 1.50 to 2.54 2.56 3.44	Random vibrations due to jet starting Model steady Small-amplitude, five-noded mode flutter at 480 to 500 cps Static bending type of failures at root Wing tore completely away at root
MW-16, MW-17, and MW-18	0.26 to 1.00 Approximately 1.70 on	Random vibrations due to jet starting Models experienced very low-amplitude vibration at 45 to 70 cps

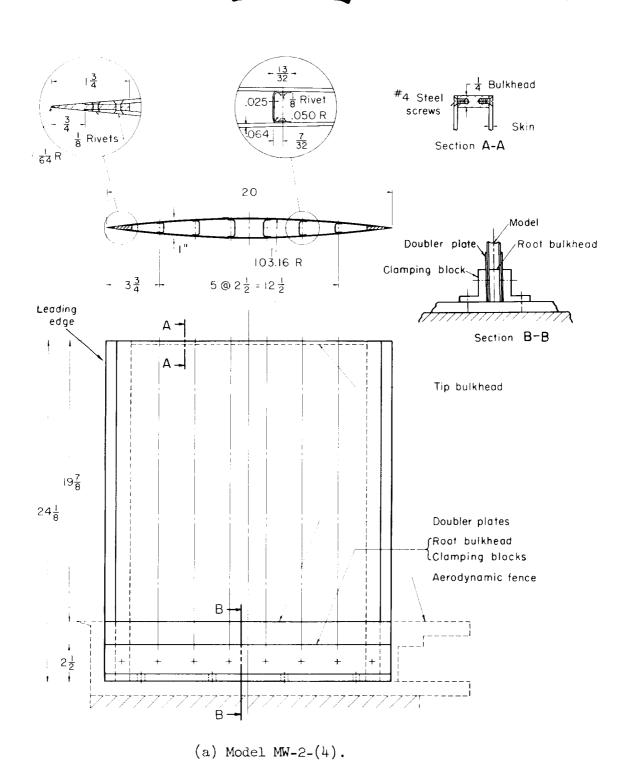
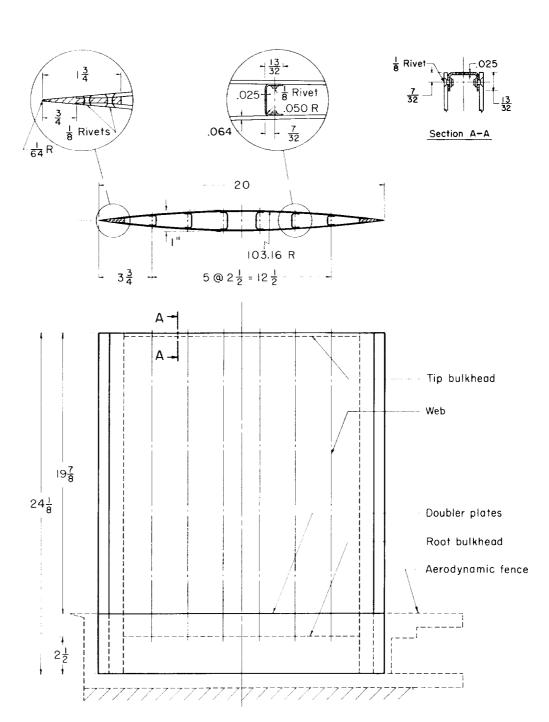


Figure 1.- Dimensions of multiweb wings.



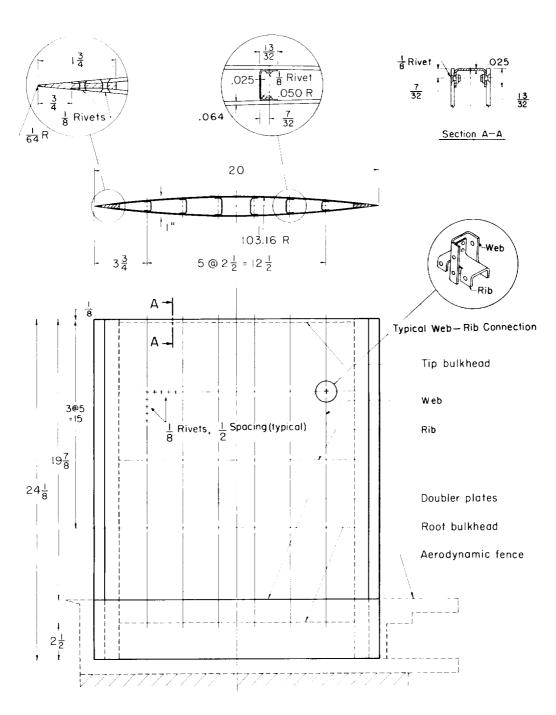


(b) Model MW-4-(3).

Figure 1.- Continued.

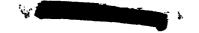


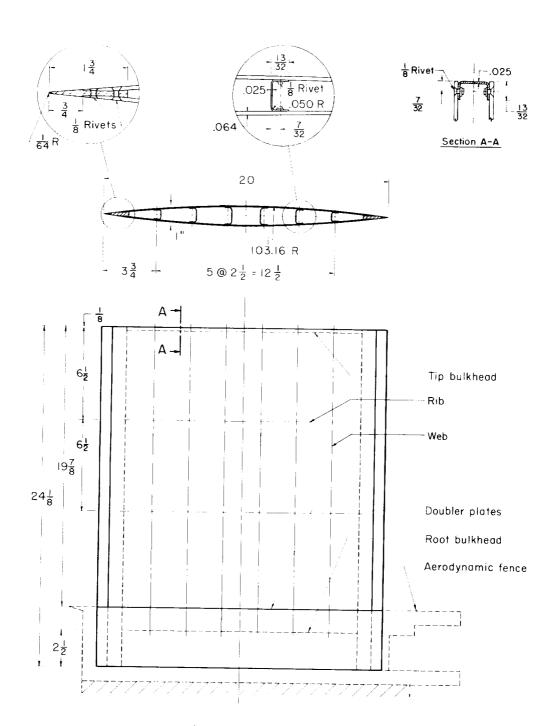




(c) Model MW-16.

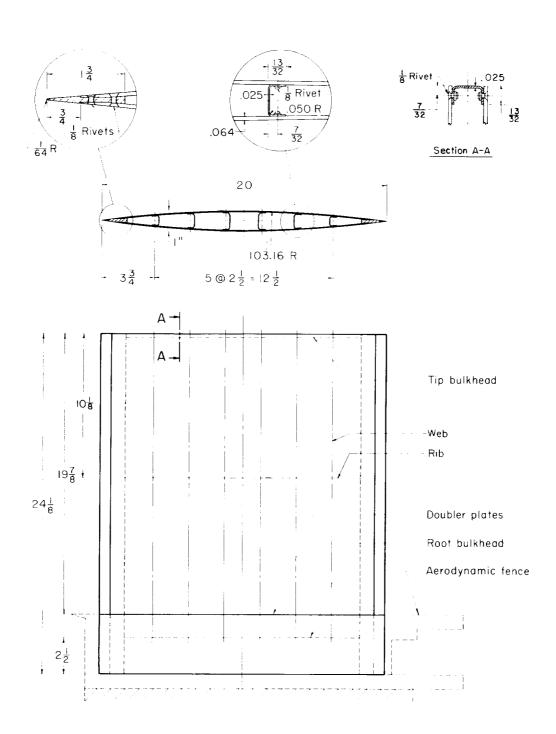
Figure 1.- Continued.





(d) Model MW-17.

Figure 1.- Continued.



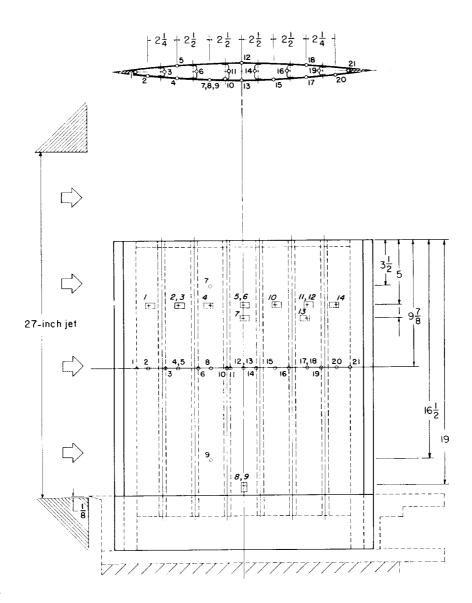
(e) Model MW-18.

Figure 1.- Concluded.

CONTRACT AT



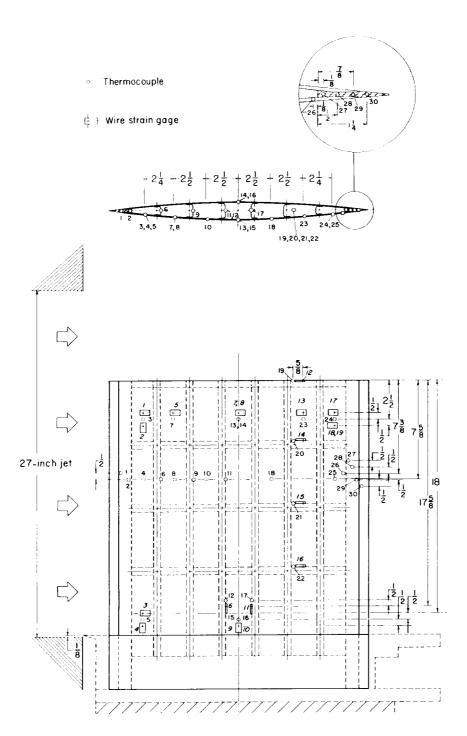
- o Thermocouple
- Wire strain gage



(a) Models MW-2-(4) and MW-4-(3).

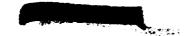
Figure 2.- Location of instrumentation for models. (Where two wire gages are listed, the second is on far skin.)



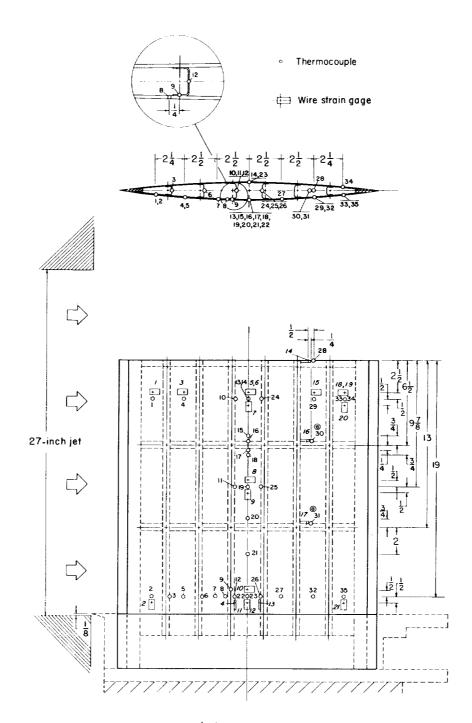


(b) Model MW-16.

Figure 2.- Continued.



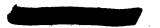




(c) Model MW-17.

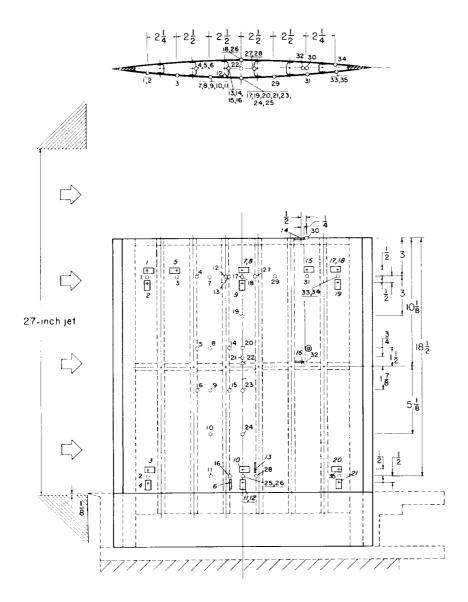
Figure 2.- Continued.





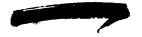
Thermocouple

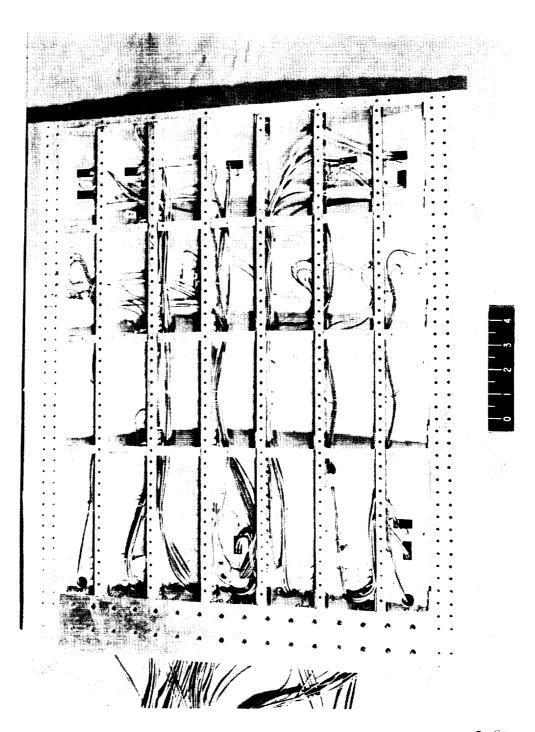
₩ire strain gage



(d) Model MW-18.

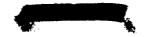
Figure 2.- Concluded.





L-80729 Figure 3.- Photograph of instrumentation of model MW-16 prior to final assembly.





		Frequency	, cps,for r	node line ^a	
Model	A	B	c	D	E
MW-2-(4)	68	147	273		351
MW_4_(3)	71	149	277		348
MW-16	5 9	148		300	
MW-17	73	I 5 5		333	
MW-18	71	152		318	
Model	F	G	H H		
MW-2-(4)	408		450		535
MW_4_(3)	392		4 30		535
MW-16		423		527	
MW_17		431		522	
MW-18		404		4 50	
Model	K		M		
Mw-2-(4)		590		665	732
MW-4-(3)	569	58 2		661	715
MW-16			668		727
MW-17			653		737
MW-18			567		740

Modes shown are composites from modes for all models.
Individual modes varied slightly from those shown.

Figure 4.- Natural frequencies and nodal patterns (A to 0) of models at room temperature.

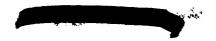
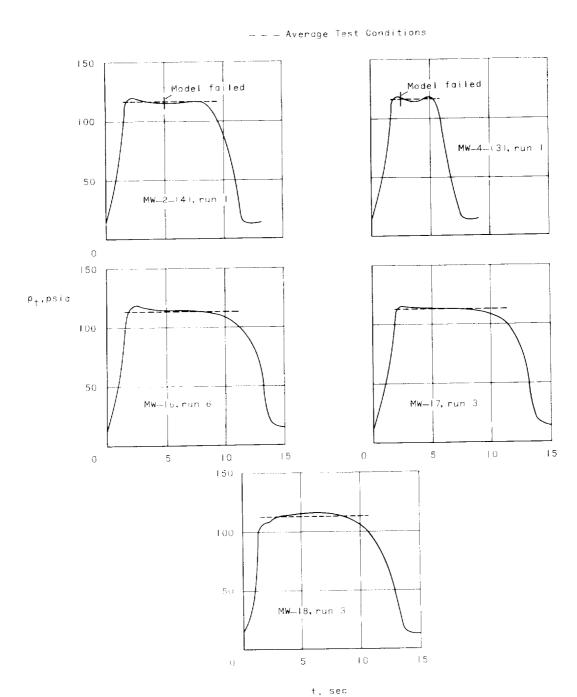




Figure 5.- Model in place at nozzle exit prior to test. L-81922





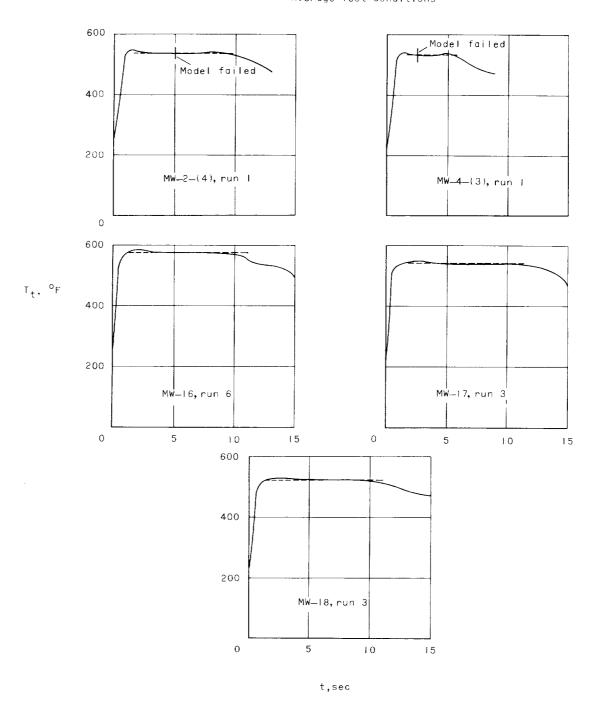


(a) Pressure.

Figure 6.- Tunnel stagnation pressure and temperature histories.



– – – Average Test Conditions



(b) Temperature.

Figure 6.- Concluded.



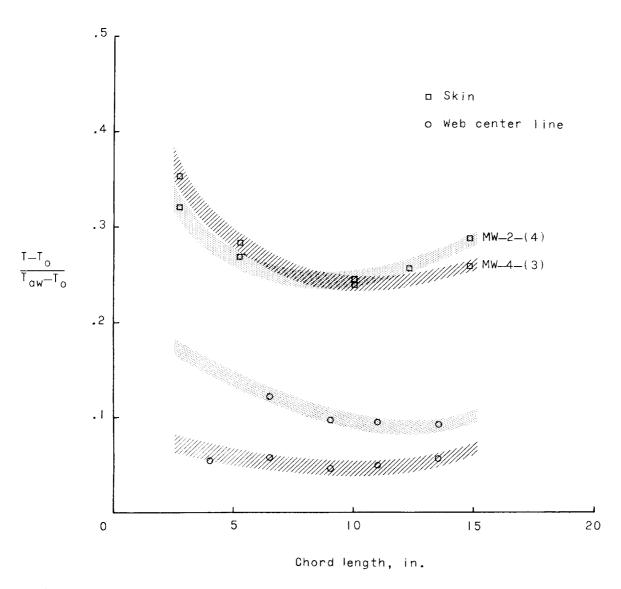


Figure 7.- Chordwise dimensionless temperatures for models MW-2-(4) and MW-4-(3) at 2 seconds.

A motion-picture film supplement, carrying the same classification as the report, is available on loan. Requests will be filled in the order received. You will be notified of the approximate date scheduled.

The film (16 mm, 10 min, B&W, silent) shows the complete tests of models MW-2-(4) and MW-4-(3) at 110 frames per second and shows sequences during the flutter and failure of these models at 1,000 or 1,600 frames per second.

Requests for the film should be addressed to the

Technical Information Division Code BIV National Aeronautics and Space Administration Washington 25, D. C.

NOTE: It will expedite the handling of requests for this classified film if application for the loan is made by the individual to whom this copy of the report was issued. In line with established policy, classified material is sent only to previously designated individuals. Your cooperation in this regard will be appreciated.

CUT

	Date
Please send TM X-186	, on loan, copy of film supplement to NASA (Film L-482).
Name of org	anization
Street numb	er
City and St Attention*	ate Mr.
	Title —————
	*To whom copy No of the TM was issued.

Place Stamp Here

Technical Information Division Code BIV National Aeronautics and Space Administration Washington 25, D. C.

CONFIDENTIAL 1. Heating, Aeredynamic (1.1.4.1) 2. Vibration and Flutter-Wings and Allerons (4.2.1) 3. Loads and Stresses, Structural - Transient Dynamic (4.3.7.7.2) I. Trussell, Donald H. II. Thomson, Rebert G. III. NASA TM X-186 NASA CONFIDENTIAL	1. Heating, Aerodynamic (1.1.4.1) 2. Vibration and Flutter Wings and Ailerons (4.2.1) 3. Loads and Stresses, Structural - Transient Dynamic (4.3.7.7.2) I. Trussell, Ontaid H. II. Thomson, Rebert G. III. NASA TM X-186 NASA CONFIDENTIAL.
NASA TM X-186 National Aeronautics and Space Administration. TESTS OF AERODYNAMICALLY HEATED MULTI- WEB WING STRUCTURES IN A FREE JET AT MACH NUMBER 2. FIVE ALUMINUM-ALLOY MODELS OF 20-INCH-CHORD WITH 0.064-INCH-THICK SKIN, 0.025-INCH-THICK WEBS, AND VARIOUS CHORD- WISE STIFFENING AT 2º ANGLE OF ATTACK. Donald H. Trussell and Robert G. Thomson. January 1960. 33p. diagrs., photos., tabs., film suppl. avail- able on request. (NASA TECHNICAL MEMORANDUM X-186) CONFIDENTIAL (Title, Unclassified) An experimental study was made on five 2024-T3 models under simulated supersonic flight conditions. One model with no internal chordwise ribs failed dynamically part way through its test; another model with no chordwise ribs experienced a static bending type of failure early in its test while undergoing flutter; and the three remaining models with one, two, Copies obtainable from NASA, Washington (over)	NASA T.M.X-186 National Aeronautics and Space Administration. TESTS OF AERODYNAMICALLY HEATED MUL II- WEB WING STRUCTURES IN A FREE JET AT MACH NUMBER 2. FIVE ALUMINUM-ALLOY MODELS OF 20-INCH-CHORD WITH 0.064-INCH-THICK SKIN, 0.025-INCH-CHORD WITH 0.064-INCH-THICK SKIN, 0.025-INCH-THICK WEBS, AND VARIOUS CHORD- WISE STIFFENING AT 20 ANGLE OF ATTACK. Donald H. Trussell and Robert G. Thomson. January 1960. 33p. diagrs., photos., tabs., film suppl. avail- able on request. (NASA TECHNICAL MEMORANDUM X-186) CONFIDENTIAL (Title, Unclassified) An experimental study was made on five 2024-T3 models under simulated supersonic flight conditions. One model with no internal chordwise ribs failed dynamically part way through its test; another model with no chordwise ribs experienced a static bending type of failure early in its test while undergoing flutter; and the three remaining models with one, two, (over)
CONFIDENTIAL 1. Heating, Aerodynamic (1.1.4.1) 2. Vibration and Flutter - Wings and Ailerons (4.2.1) 3. Loads and Stresses, Structural - Transient Dynamic (4.3.7.7.2) I. Trussell, Donald H. II. Thomson, Robert G. III. NASA TM X-186 NASA CONFIDENTIAL	CONFIDENTIAL 1. Heating, Aerodynamic (1.1.4.1) 2. Vibration and Flutter - Wings and Alierons (4.2.1) 3. Loads and Stresses, Structural - Transient Dynamic (4.3.7.7.2) I. Trussell, Donald H. II. Thomson, Rebert G. III. NASA TM X-186 NASA CONFIDENTIAL.
NASA T.M. X-186 National Aeronautics and Space Administration. TESTS OF AERODYNAMICALLY HEATED MULTI- WEB WING STRUCTURES IN A FREE JET AT MACH NUMBER 2. FIVE ALUMINUM-ALLOY MODELS OF 20-INCH-THICK WEBS, AND VARIOUS CHORD- WISE STIFFENING AT 2° ANGLE OF ATTACK, Donald H. Trussell and Robert G. Thomson. January 1960. 33p. diagrs., photos., tabs., film suppl. avail- able on request. (NASA TECHNICAL MEMORANDUM X-186) CONFIDENTIAL (Title, Unclassified) An experimental study was made on five 2024-T3 models under simulated supersonic flight conditions. One model with no internal chordwise ribs failed dynamically part way through its test; another model with no chordwise ribs experienced a static bending type of failure early in its test while undergoing flutter; and the three remaining models with one, two, Copies obtainable from NASA, Washington	NASA TM X-186 National Aeronautics and Space Administration. TESTS OF AERODYNAMICALLY HEATED MULTI- WEB WING STRUCTURES IN A FREE JET AT MACH NUMBER 2. FIVE ALUMINUM-ALLOY MODELS OF 20-INCH-CHORD WITH 0.064-INCH-THICK SKIN, 0.025-INCH-CHORD WITH 0.064-INCH-THICK SKIN, 0.025-INCH-THICK WEBS, AND VARIOUS CHORD- WISE STIFFENING AT 20 ANGLE OF ATTACK. Donald H. Trussell and Robert G. Thomson. January 1960. 33p. diagrs., photos., tabs., film suppl. avail- able on request. (NASA TECHNICAL MEMORANDUM X-186) An experimental study was made on five 2024-T3 models under simulated supersonic flight conditions. One model with no internal chordwise ribs failed dynamically part way through its test; another model with no chordwise ribs experienced a static bending flutter; and the three remaining models with one, two, (over)

The second secon			
NASA TM X-186 or three chordwise ribs between root and tip survived their tests.	CONFIDENTIAL	NASA TM X-186 or three chordwise ribs between root and tip survived their tests.	CONFIDENTIAL
Copies obtainable from NASA, Washington	NASA CONFIDENTIAL	Copies obtainable from NASA, Washington	NASA CONFIDENTIAL
NASA TM X-186 or three chordwise ribs between root and tip survived their tests.	CONFIDENTIAL	NASA TM X-186 or three chordwise ribs between root and tip survived their tests.	CONFIDENTIAL
	NASA		ASAM
Copies obtainable from NASA, Washington	CONFIDENTIAL	Copies obtainable from NASA, Washington	CONFIDENTIAL